Electronic Supplementary Material for

Electric-field-induced deformation, yielding, and crumpling of jammed particle shells formed on non-spherical Pickering droplets

K. Khobaib,[a] A. Mikkelsen,[a] T. Vincent-Dospital,[b] and Z. Rozynek[a,b*]

[a] Faculty of Physics, Adam Mickiewicz University, Uniwersytetu Poznańskiego 2, 61-614 Poznań, Poland

[b] PoreLab, The Njord Centre, Department of Physics, University of Oslo, P. O. Box 1048, Blindern, N-0316 Oslo, Norway

Fig. S1 demonstrates the creation of homogeneous and non-homogeneous arrested Pickering droplets by droplet coalescing. Two silicone oil droplets partly covered with particles coalesced to form an arrested Pickering droplet. The shape of the final coalesced droplet is determined by the particle surface coverage of the two original droplets. In **Fig. S1**, the particle concentration of the original droplets varied from ~8 to ~12 wt.%. As a result, we obtained Pickering droplets of different shapes, including a spherical shape (**Fig. S1a**), a slightly aspherical shape (**Fig. S1b**), a rectangle-like shape (**Fig. S1c**), and a peanut-like shape (**Fig. S1d**). The coalesced droplet in **Fig. S1a** was not completely covered with particles (two openings can be seen at the electric poles of the droplet). That is, the particle layer was not in a jammed state, and the particles had some space available to rearrange. The other coalesced Pickering droplets had jammed particle layers that kept the droplet in a non-spherical shape also after the *E*-field was turned off. Owing to particle rigidity (the particles cannot be deformed, and it costs energy to move particles out of plane), the particle layer resisted the retracting force stemming from the surface tension of the droplet.

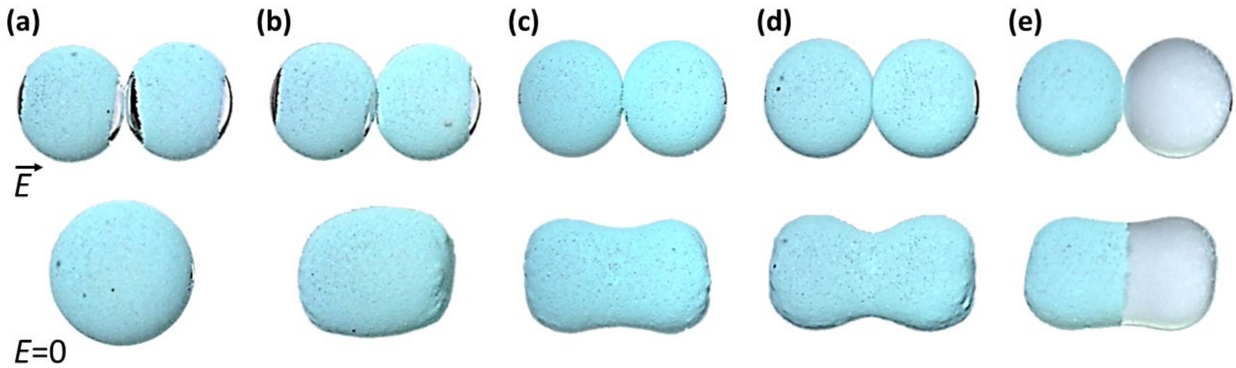

Fig. S1. Pickering droplets with different shapes made by electrocoalescence. The droplets just before electrocoalescence are presented in the top row, whereas the coalesced droplets are shown in the bottom row. The original particle concentrations on the two original droplets were **(a)** ~8 wt%, **(b)** ~9 wt%, **(c)** ~10 wt%, and **(d)** ~11 wt%. Blue 30-µm PE particles were used to form homogenous shells **(a-d)**. **(e)** An example of a Janus shell composed of PE particles of two different sizes: blue 30-µm PE particles and white 2-µm particles. The original particle concentrations of the two original droplets were ~10 and ~12 wt% for the blue and white particles, respectively. The size of each original droplet was ~ 2.0 mm. See also corresponding **Movie S1**.

Fig. S2 demonstrates that at a weak *E*-field (350 V mm^{-1}), droplets deformed from a prolate into an oblate shape without an observable formation of wrinkles at their particle shells or with irregular folds with small amplitudes. Slow compression of particle shells facilitated in-plane particle rearrangement analogous to the gliding of grain layers in granular flows. In response to compressive electric stress, the surface particles started to move relative to one another. We observed several slip lines appearing during shell compression.

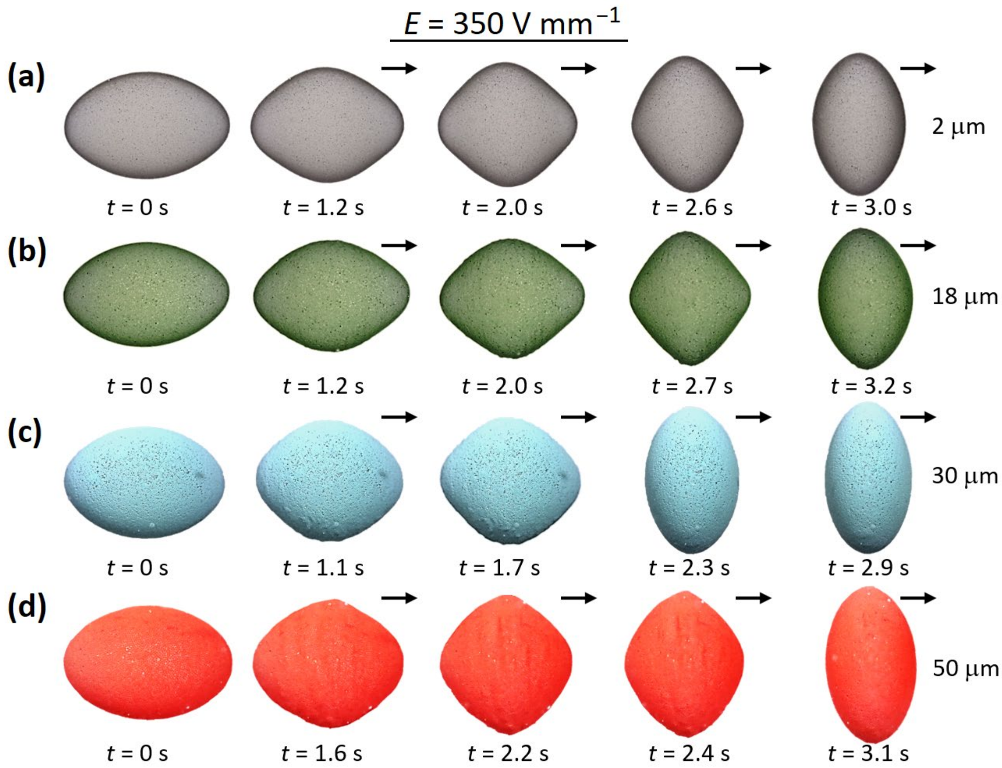

Fig. S2. Deformation of particle shells at different *E*-field strengths. Arrested droplets with PE particle shells made of **(a)** 2-µm, **(b)** 18-µm, **(c)** 30-µm and **(d)** 50-µm PE particles. Initially, at *t* = 0 s, the particle shells were ellipsoidal with a major axis of 3.9 mm and a minor axis of 2.6 mm. Electric field applied in horizontal direction.

In **Fig. S3**, we show that depending on the compression dynamics (i.e., *E*-field strength) the particle-covered droplets undergo different shape transformations at the intermediates during the prolate-to-oblate shape transition. The difference between the droplets' projected two-dimensional (2D) shapes is clearly seen (especially in the middle column of the figure. The contours of the Pickering droplets subjected to the weakest *E*-field (350 V mm^{-1}) resembles a rhombus shape, whereas that of the Pickering droplet subjected to the strongest E-field (1050 V mm^{-1}) are nearly spherical.

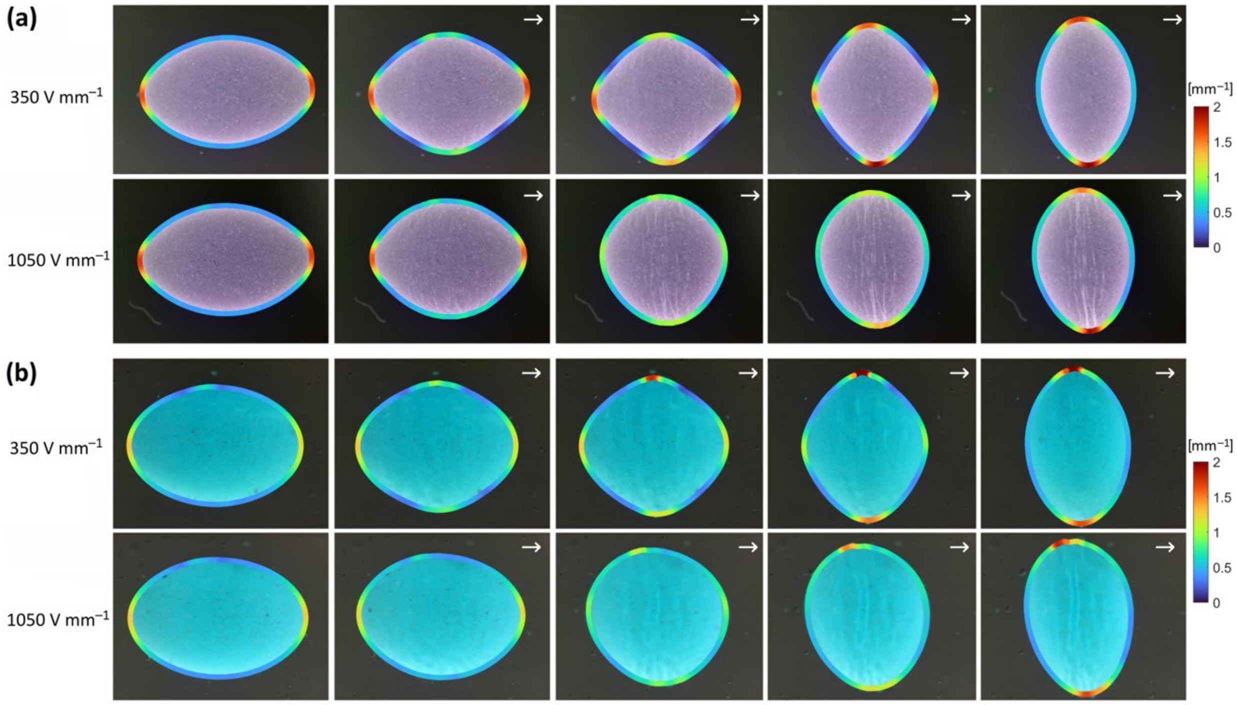

Fig. S3. Deformation of particle shells at different *E*-field strengths. Series of experimental images with added color-coded contours representing values of the curvature. Arrested droplets with particle shells made of **(a)** 18 µm and **(b)** 50 µm particles. The droplets were subjected to *E*-fields of strengths 350 and 1050 V mm^{-1}. The droplets subjected to the stronger *E*-field are more round at the intermediates compared to those subjected to the weak *E*-field. Note: The Pickering droplet with 50 µm particles wrinkles with the wrinkling amplitude of several pixels, which was picked up by the software that affected the shape of the contours.

Movie S1. Collection of movies demonstrating the preparation of Pickering droplets with different shapes. In each movie, two silicone oil droplets with surface particles undergo electrocoalescence subjected to a DC *E*-field of strength 170 V mm^{-1}. The resultant shape of the droplet depends on the initial particle coverage. The movie is sped up 2 times.

Movie S2. Preparation of ellipsoidal particle shells by using DC and AC *E*-fields. An ellipsoidal particle shell is prepared by the electrorotation of a Pickering droplet in a DC *E*-field, followed by the aligning of the droplet (with its longest axis along the direction of the *E*-field) and the shaping of the droplet using an AC *E*-field (100 Hz).

Movie S3. *E*-field-induced deformation of arrested droplets with jammed particle shells. A silicone oil droplet covered with 30-µm PE particles was suspended in castor oil and subjected to a DC *E*-field that was stepwise increased. The applied *E*-field and the deformation of the droplet are plotted against time.

Movie S4. Particle in-plane rearrangement. Droplets with shells made of 2 µm, 30 µm, and 100 µm PE particles under electric stress. Each movie is recorded with a reverse playback and is sped up two times.

Movie S5. Deformation of non-spherical Pickering droplets subjected to different *E*-field strengths. Three arrested droplets (with similar volume and initial shape) covered by 2-µm PE particles are subjected to *E*-fields of strengths 350, 700, and 1050 V mm^{-1}. Under these *E*-field strengths, the droplets continuously deformed from prolate into oblate shapes but with different dynamics.

Movie S6. Crumpling of particle shells. Four droplets covered by PE particles of different diameters 2–50 µm were subjected to *E*-field of strength 1050 V mm^{-1}. Initially, at $t = 0$ s, the particle shells were ellipsoidal with a major axis of ~3.9 mm and a minor axis of ~2.6 mm. The movies were slowed down four times.

Movie S7. Shape transformations of a Pickering droplet under different speed of compression. Arrested droplets (with similar volume and initial shape) covered by 2-µm PE particles were subjected to *E*-fields of strengths 350–1050 V mm^{-1}. Series of experimental images with added color-coded contours representing values of the curvature are shown on the top row. The estimated curvature values are plotted against the 2D polar angle, and the curvature distributions are presented using bar charts.

Movie S8. Asymmetric Pickering droplets under electrical stress. A homogeneous particle shell is prepared by the coalescence of 1.6- and 2.7-mm silicone oil droplets covered with blue 30-µm PE particles. Three different types of heterogeneous particle shells are prepared by the coalescence of silicone oil droplets covered with white 2-µm and red 50-µm PE particles, and green 100-µm and white 2-µm PE particles. The asymmetrical particle shells are subjected to an *E*-field of strength ~300 V mm^{-1}.

MATLAB code

```
% Curvature computation around a Pickering Droplet / Matlab Code

clc; clear; close all

%% Extra function (index wrapping)
wrapN = @(x, n) (1 + mod(x-1, n));

%% Parameters
image_file = 'name.jpg';
T = 0.41; % Threhold for the detection of the droplet's boundary (0<T<1)
sm = 20; % Number of points for the average smoothing filterering of the boundary
k = 50; % Number of data points to fit local circles to the boundary

%% Charge image and compute droplet boundary
I = imcomplement(imread(image_file));
% imshow(I)
BW = im2bw(I,T);
% imshow(BW)

dim = size(BW);
col = round(dim(2)/2)-90;
row = min(find(BW(:,col)));
boundary = bwtraceboundary(BW,[row, col],'N');

%%% Smoothing
boundary(:,2) = smooth(boundary(:,2),sm);
boundary(:,1) = smooth(boundary(:,1),sm);

%% Compute curvature
n = length(boundary(:,2));
curv = NaN*zeros(1,n);

%%% Fitting Circles, Kasa Method (1976)
for i=1:n
  if ((i+k <= n) && (i-k >= 1))
    [xc,yc,R] = Kasa(boundary(i-k:i+k,2),boundary(i-k:i+k,1));
  elseif i+k > n
    [xc,yc,R] = Kasa([boundary(i-k:n,2);boundary(1:wrapN(i+k,n),2)],[boundary(i-
k:n,1);boundary(1:wrapN(i+k,n),1)]);
  elseif i-k < 1
    [xc,yc,R] = Kasa([boundary(wrapN(i-k,n):n,2);boundary(1:i+k,2)],[boundary(wrapN(i-
k,n):n,1);boundary(1:i+k,1)]);
  end
  curv(i)=1/R;
end

%%% Conversion to mm
pixsize = 0.00405;
curv = curv/pixsize;

%% Ploting
figure(1)
set(gcf, 'Position', get(0, 'Screensize'));
set(gcf,'color','w');

subplot(1,3,1)
imshow((I))
hold on;
scatter(boundary(:,2),boundary(:,1),20,curv,'filled');
colorbar
```

```
colormap('turbo')
caxis([0,2])
title({'Approximate curvature (mm^{−1})'})

%%% QCing the last fitted circle
% hold on
% viscircles([xc yc],R);

xc=mean(boundary(:,2)); yc=mean(boundary(:,1));
Theta=atan2(-(boundary(:,1)-yc),(boundary(:,2)-xc)) ;
subplot(1,3,2)
polarplot(Theta,curv,'linewidth',2)
rlim([0 0.008/pixsize])
title('Polar plot of the curvature (mm^{−1})')

subplot(1,3,3)
h1=histogram(curv,'FaceAlpha',1,'Normalization','probability');
h1.BinWidth = 0.0001/pixsize;
xlim([0,0.008/pixsize]) ; ylim([0.003,0.3]) ;
set(gca,'YScale','log')
title('Curvature probability distribution (mm^{−1})')

%% Extra functions
function   [xcenter,ycenter,radius] = Kasa(xdata,ydata)

%     I. Kasa, "A curve fitting procedure and its error analysis",
%     IEEE Trans. Inst. Meas., Vol. 25, pages 8-14, (1976)

  Mat=[xdata ydata ones(size(ydata))]\[-(xdata.^2+ydata.^2)];
  xcenter = -Mat(1)/2;
  ycenter = -Mat(2)/2;
  radius  =  sqrt((Mat(1)^2+Mat(2)^2)/4-Mat(3));

end
```